The 9th European Congress on Computational Methods in Applied Sciences and Engineering
ECCOMAS Congress 2024
3–7 June 2024, Lisboa, Portugal

LEVEL 2-CALCULATIONS OF DYNAMIC VEHICLE-BRIDGE COMPATIBILITY FOR DETERMINING PERMISSIBLE SPEEDS IN THE RAILWAY NETWORK (GERMANY)

RONNY BEHNKE[1], GÜNTHER GRUNERT[1] AND XIAOHAN LIU[1]

[1] DB InfraGO AG
10115 Berlin, Germany
e-mail: ronny.behnke@deutschebahn.com

Key words: Dynamics, Train-Bridge Compatibility, Limit Velocity, Damping, Fatigue, Acceleration

Summary. As part of the network access process for new railway vehicles, the static and dynamic compatibility between the vehicle and existing bridges must be evaluated. For high-speed railway vehicles in particular, dynamic bridge compatibility is one of the factors determining the maximum admissible vehicle speed on the railway network. Bridge compatibility includes vehicle-specific bridge verifications within the framework of the ultimate limit state (ULS) and the serviceability limit state (SLS). The verification procedure is divided into Levels 1 to 5, which are characterized by increasing complexity of the verification process. In Levels 1 and 2, simple parameter studies are used to verify and demonstrate the compatibility for the entire network. Levels 3 to 5 are implemented on a line-by-line basis by computing results on individual line structures. The objective of this contribution is to extend the verification process in Level 2 regarding the modeling of damping and fatigue (ULS) as well as acceleration (SLS) by also studying different load-bearing systems occurring in the network. The dynamic properties of the bridge stock (network) are represented by conservative assumptions of the system variables. For this purpose, new evaluations of the information available from measurements and construction documents of bridges were carried out (distributed mass, eigenfrequency, damping) representing the railway bridge network in Germany (DB InfraGO AG). As part of the new parameter studies, the influence of non-linear damping on the response spectrum for different spans is investigated (velocity-dependent, displacement-dependent damping) and compared with each other. In combination with a subsequent study of the vehicle stock of current vehicles and new vehicle developments, the verification method shown in this contribution will be employed in the future for the revision of the vehicle type-specific static/dynamic speed limits (DIN EN 15528:2022, Table C.1) as part of the EU project InBridge4EU at European level.

1 INTRODUCTION

New trains (vehicles) must be examined for dynamic compatibility with the existing bridge infrastructure during the network access process. At higher speeds, bridge decks can be excited to significant vibrations by the repeated, regular sequence of wheelset/axle loads when trains pass over them, see e.g. [5, 8]. This phenomenon occurs when one of the excitation frequencies from train passage is close to the natural frequencies of the respective bridge structure (resonance

case). The effects on the bridge infrastructure are to be investigated with regard to the ultimate limit state (ULS) and the serviceability limit state (SLS). Effects of fatigue (FAT) must be taken into account, see e.g. [2].

The assessment procedure for new vehicles (in Germany) is divided into 5 levels and described in more detail in [3]. In Fig. 1, Levels 1 to 5 are illustrated in relation to the level of detail (LoD) of the train-bridge-infrastructure model considered in each case. The objective is to confirm the vehicle design speed to be achieved as the base speed (network access) for the entire railway network as early as possible in Levels 1 and 2 by means of bridge dynamics investigations. This permissible speed (Level 2) is referred to as the so-called base speed per infrastructure line category (LC), here used as available capacity of the railway network. The challenge is that in Level 2, compatibility is carried out using parameter studies on a representative set of bridges (single-span girders) for which conservative assumptions (natural frequency, distributed mass of the bridge deck, damping) are used. The parameter study should be representative of the bridge stock in the overall railway network. The most common structural system in Germany (DB InfraGO AG) is the single-span girder, see [4] for a review of high-speed railway bridges in Germany. Continuous girders are included to a certain extent due to their resonant lengths L_Φ. For special structures, the results of the parameter study are only meaningful to a limited extent, separate investigations (in Level 3 and higher) are necessary in these cases.

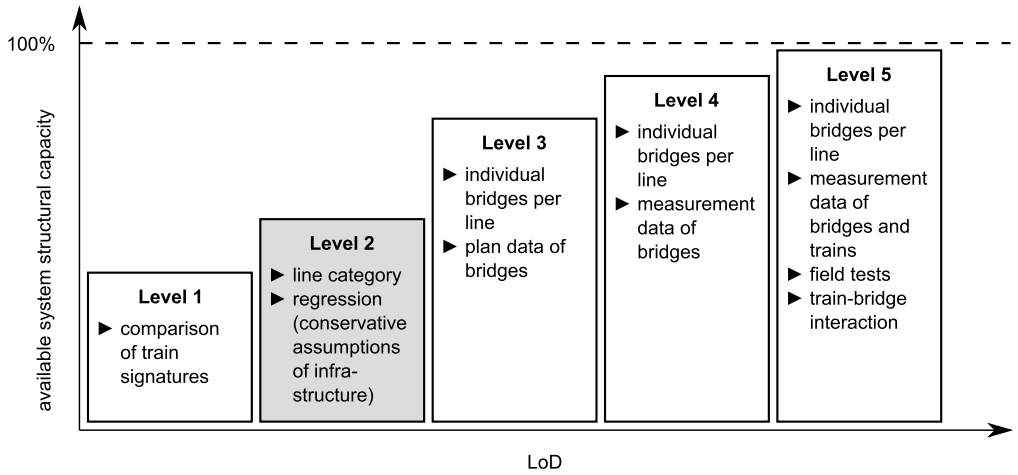

Figure 1: Levels of verification (see [3]) as a function of the levels of detail (LoD) for the network access process of new vehicles/trains exceeding permissible limit speeds of quasi-static compatibility given in DIN EN 15528:2022, Table C.1

The conservative properties for describing the existing infrastructure as part of the parameter study can be taken from measured values of existing bridges (distributed mass, damping ratio) or lower limits provided in construction standards (limit lines of natural frequency, damping as a function of the construction type). As a starting point, the current implementation status takes linear material and linear structural behavior into account. The aim is to extend the existing method to include non-linear damping effects (increased damping in the event of resonance). Taking non-linearities into account is not standard so far, see e.g. [7], but will be limited in the following to physical non-linearities, i.e. the structures are assumed to stay in the geometrical linear range during operation.

2 INFRASTRUCTURE DATA

As described in the introduction, the following input parameters (linear calculation – L) of the following form are currently required for the description of the existing bridge infrastructure:

- static system (assumption: single-span girder in the span range $1\,\mathrm{m} \leq L \leq 120\,\mathrm{m}$) modeled as a simply supported beam (Euler-Bernoulli beam theory),
- natural frequency (assumption: lower frequency line $n_{02}(L)$ of DIN EN 1991-2:2010 as a function of the span L),
- distributed mass (assumption: 5%-fractile for each construction type taken from plan data for current bridge stock as a function of the span L for bridge structures whose calculated first natural bending frequency is $n_0(L) \leq 0.8\,n_{02}(L) + 0.2\,n_{01}(L)$, see Fig. 2, where $n_{01}(L)$ is the upper frequency line specified in DIN EN 1991-2:2010),
- damping ratio (assumption: standard damping specified in DIN EN 1991-2:2010 for each construction type with consideration of the additional damping (DIN EN 1991-2:2010) from train-bridge interaction as a function of the span L).

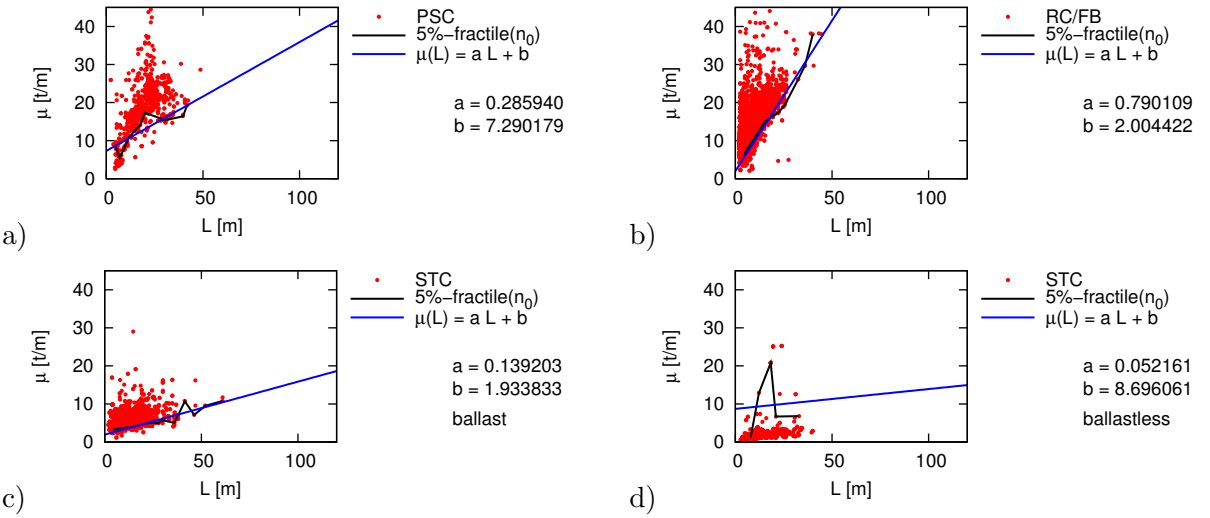

Figure 2: Calculated distributed mass (5%-fractile value per range of span length L) from plan information for the railway bridge population at DB InfraGO AG (Germany), frequency condition used for regression $n_0(L) \leq 0.8\,n_{02}(L) + 0.2\,n_{01}(L)$: PSC – pre-stressed concrete, RC/FB – reinforced concrete / filler beam, STC – steel/composite

In the following, non-linear effects resulting from increased damping values, e.g. at large amplitudes, are also to be recorded (non-linear calculation – NL). For this purpose, dynamic measurement series of passing trains on a total of 716 bridge decks of different construction types (reinforced concrete / filler beam: 192, pre-stressed concrete: 116, steel/composite: 408) were evaluated and the average value and the 95%-fractile value of the damping ratio D (free decay phase) per bridge deck were determined from each bridge measurement series, see Fig. 3.

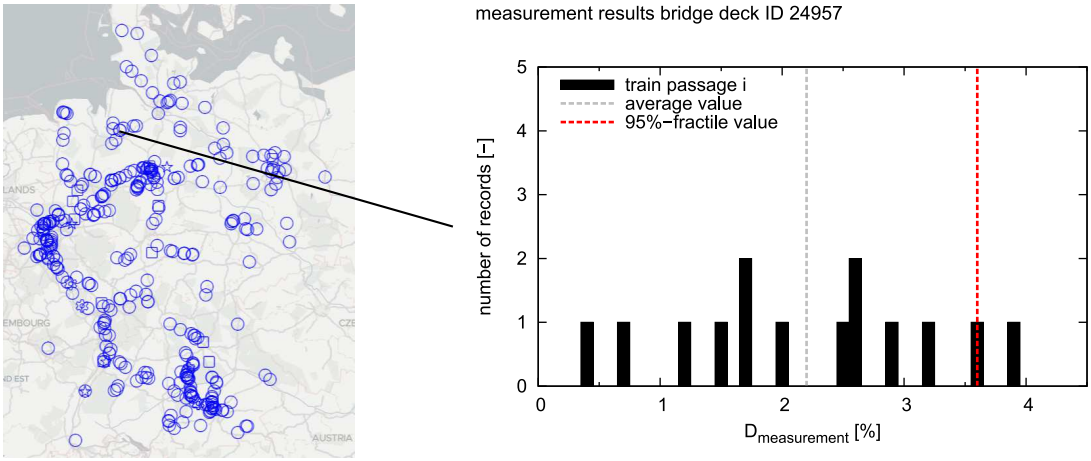

Figure 3: Railway bridge decks with dynamic measurements (Germany) with identified damping ratios D (decay phase) per train passage (measurement series of one bridge exemplarily depicted as histogram)

For comparison, the determined damping ratios are shown in normalized form in relation to the damping values specified in DIN EN 1991-2:2010 in Fig. 4 (without additional damping stemming from train-bridge interaction). For the algorithmic implementation of the damping ratio as a function of the considered bridge length L, a linear regression function with the input parameter L was calculated for the average values and 95%-fractile values determined from the measurement data. If the level of knowledge is sufficiently precise, other approach functions (polynomial regression) or mapping via model-free approaches (machine learning) are also conceivable.

Figure 4 shows that both regression lines are above the normative limit value D_{norm} (damping according to DIN EN 1991-2:2010) for all construction types. Applying the 95%-fractile values for the damping ratio will result in higher damping values for each construction type at significantly large amplitudes, i.e. at resonance. In the next section, a non-linear damping model is proposed that uses the lower damping values from DIN EN 1991-2:2010 as a basis and applies higher damping values with increasing vibration amplitudes up to an upper limit value. For the upper limit value, the 95%-fractile value for the damping ratio (regression function) is used in the following.

In addition to the measured values for the damping ratios shown in Fig. 4, measured values for the natural frequency of the bridges are also available. These are not used any further in the following investigation.

3 LEVEL 2-TRAIN-BRIDGE MODEL

As introduced in Sec. 2, the input parameters were used for the generation of representative bridge models subjected to train passage (numerical finite element (FE) simulation), see Fig. 5. The gradation of the span L are based on the step sizes per span range proposed in DIN EN 15528:2022 (finer step size for smaller spans, coarser step size for larger spans). The action induced by train passage is represented by a moving load model of the static wheelset loads (axle loads) in the mass state MND (mass normal payload for dynamic calculations) at train velocity v. Here, individual axle loads (single forces) are considered as longitudinally three-point-

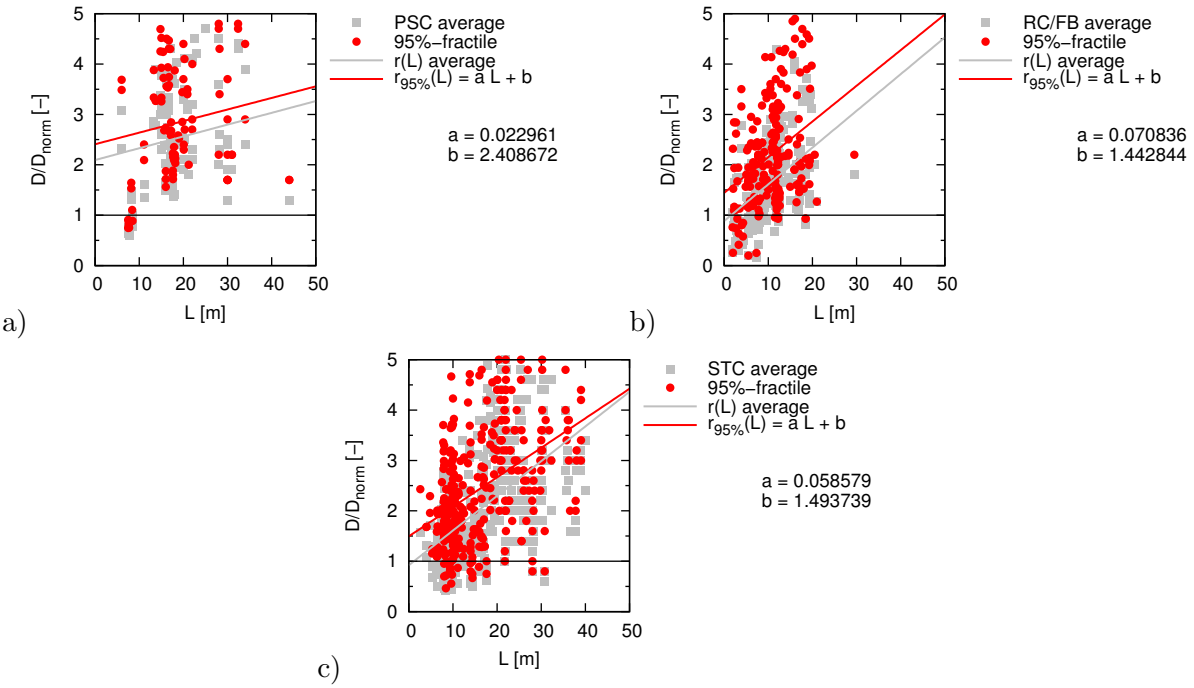

Figure 4: Normalized damping ratio (average value, 95%-fractile value) identified from measurement series of different bridges with span L at DB InfraGO AG (Germany): PSC – pre-stressed concrete, RC/FB – reinforced concrete / filler beam, STC – steel/composite

distributed (three single forces) according to DIN EN 1991-2:2010 (sleeper spacing $a = 0.60\,\mathrm{m}$).

The natural frequency $n_{02}(L)$ (lower frequency line of DIN EN 1991-2:2010) is assigned to the considered span L of the bridge model and the associated bending stiffness EI is calculated by using the mass assignment $\mu_{5\%}(L)$ shown in Fig. 2 (regression line of the 5%-fractile values),

$$EI(L) = \frac{4\, n_{02}(L)^2\, \mu_{5\%}(L)\, L^4}{\pi^2}\,. \tag{1}$$

Regarding the damping ratio D within linear calculations (L), constant, lower values are applied according to DIN EN 1991-2:2010 ($D_{\mathrm{norm}}(L)$). For the non-linear calculation (NL), the following damping model $D_{\mathrm{NL}}(q_i, L)$ is assumed as a function of the degree of freedom (DOF) q_i of the modal space (eigenmodes). The scalar approach for the mode shape i is shown in Fig. 6. The tanh-function is used as qualitative shape function for the interpolation of the lower limit value $D_{\mathrm{norm}}(L)$ and the upper limit value $D_{95\%}(L)$,

$$D_{\mathrm{NL}}(q_i, L) = \left[1 + \left(\frac{D_{95\%}(L)}{D_{\mathrm{norm}}(L)} - 1\right) \tanh(s\ \mathrm{abs}(q_i))\right] D_{\mathrm{norm}}(L)\,, \tag{2}$$

where s is a scaling factor to be selected as a function of experimental measurements (definition of the amplitude level of DOFs q_i).

The scalar damping model given in Eq. (2) is transformed for the entire structure with the structural DOF $\mathbf{u}$ using the matrix of eigenvectors $\mathbf{X}$ of the undamped system,

$$\mathbf{u}(t) = \mathbf{X}\,\mathbf{q}(t)\,, \tag{3}$$

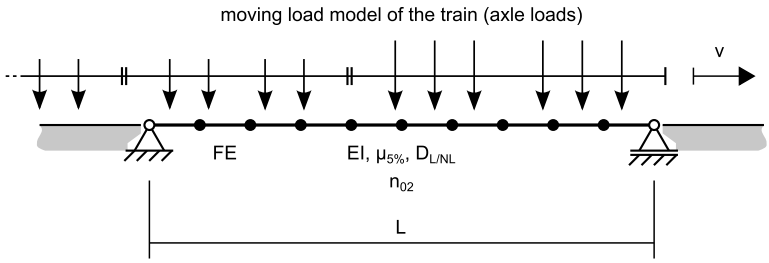

Figure 5: Moving load model (train with axle loads) on FE discretized bridge (simply supported beam)

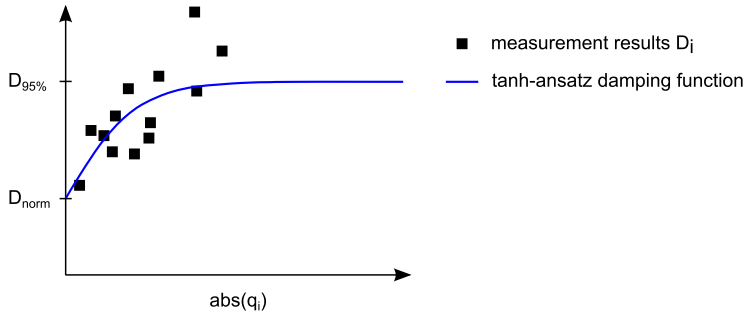

Figure 6: Non-linear damping model (qualitative form)

where the vector of the system's DOF is $\mathbf{u}(t)$ and the vector of the system's modal DOF is $\mathbf{q}(t)$. The special construction of the system's damping matrix $\mathbf{D}$ from the system's modal damping matrix

$$\mathbf{X}^{\mathrm{T}}\,\mathbf{D}\,\mathbf{X} \stackrel{!}{=} \mathrm{diag}\{d_{gi}\} = \mathrm{diag}\{2\,m_{gi}\,\omega_{\mathrm{E}i}\,D\} \tag{4}$$

yields its definition with respect to the system's DOF

$$\mathbf{D} = \mathbf{X}^{-\mathrm{T}}\;\mathrm{diag}\{d_{gi}\}\;\mathbf{X}^{-1} \tag{5}$$

where to each mode i, a damping coefficient

$$d_{gi} = 2\,m_{gi}\,\omega_{\mathrm{E}i}\,D \tag{6}$$

is attributed, where m_{gi} is the general mass of mode i, $\omega_{\mathrm{E}i}$ is the ith circular eigenfrequency of the undamped system and D is the damping ratio taken as $D_{\mathrm{norm}}(L)$ in the case of the linear calculation (L) or $D_{\mathrm{NL}}(q_i, L)$ in the case of the non-linear calculation, see Eq. (2).

As part of the time history calculation (see next section), the amplitude for each eigenmode is first calculated using the inverse relation of Eq. (3)

$$\mathbf{q}(t) = \mathbf{X}^{-1}\,\mathbf{u}(t) \tag{7}$$

and the equation of motion is solved iteratively. The matrix $\mathbf{X}$ of eigenvectors is obtained by solving the general eigenvalue problem given by the system's matrices $\mathbf{K}$ and $\mathbf{M}$ with implemented boundary conditions. The matrices $\mathbf{K}$ (stiffness matrix) and $\mathbf{M}$ (mass matrix) are generated by assembling the element matrices of the linear 2D displacement elements (2 displacement DOF and 1 rotational DOF per node) used for geometrical discretization of the bridge

deck, see Fig. 5. The assembling process is carried out once at the start of the calculation for span L. The damping matrix is constant in the case of the linear calculation (L). In the case of the non-linear calculation (NL), the damping matrix is recalculated in each time step and in each iteration as a function of the amplitudes of the bridge vibration.

4 NEWMARK TIME-INTEGRATION SCHEME

For calculating the dynamic response of the bridge structure, the FE-discretized system depicted in Fig. 5 is numerically solved with the Newmark time-integration scheme as outlined in the following. The Newmark time-integration scheme, see e.g. [1], uses the following assumptions for velocity

$$\dot{\mathbf{u}}_{t+\Delta t} = \dot{\mathbf{u}}_t + \left[(1-\delta)\,\ddot{\mathbf{u}}_t + \delta\,\ddot{\mathbf{u}}_{t+\Delta t}\right]\Delta t \tag{8}$$

and displacement

$$\mathbf{u}_{t+\Delta t} = \mathbf{u}_t + \dot{\mathbf{u}}_t\,\Delta t + \left[\left(\frac{1}{2}-\alpha\right)\ddot{\mathbf{u}}_t + \alpha\,\ddot{\mathbf{u}}_{t+\Delta t}\right]\Delta t^2 \tag{9}$$

at time $t+\Delta t$. Quantities from time t (previous known solution point) are also involved in this expression (time domain). The time step Δt is kept constant during the solution of one given bridge system of span L. The time step size is computed at the beginning of the calculation from the criteria to best resolve the eigenfrequency of the bridge deck (free decay phase, see e.g. [6]) or the passage of the train for the given velocity v. The parameters

$$\delta \geq \frac{1}{2}\,, \quad \alpha \geq \frac{1}{4}\left(\frac{1}{2}+\delta\right)^2 \tag{10}$$

are known to govern the numerical stability of the computation scheme and represent weighting factors for the quantities at time t and $t+\Delta t$, see Eqs. (8) and (9). For time $t+\Delta t$, the equation of motion becomes in time-discretized form

$$\mathbf{M}\,\ddot{\mathbf{u}}_{t+\Delta t} + \mathbf{D}\,\dot{\mathbf{u}}_{t+\Delta t} + \mathbf{K}\,\mathbf{u}_{t+\Delta t} = \mathbf{R}_{t+\Delta t}\,, \tag{11}$$

where $\mathbf{M}$ is the mass matrix, $\mathbf{D}$ represents the damping matrix and $\mathbf{K}$ is the stiffness matrix of the FE-discretized system (see Fig. 5) at time $t+\Delta t$. Note that for the geometrically linear system, $\mathbf{M}$ and $\mathbf{K}$ are always constant over time, whereas $\mathbf{D}$ is only constant for the linear calculation. $\mathbf{R}_{t+\Delta t}$ stands for the nodal force vector evaluated at time $t+\Delta t$. With the help of the abbreviations

$$a_0 = \frac{1}{\alpha\,\Delta t^2}\,, \quad a_1 = \frac{\delta}{\alpha\,\Delta t}\,, \quad a_2 = \frac{1}{\alpha\,\Delta t}\,, \quad a_3 = \frac{1}{2\,\alpha} - 1\,, \tag{12}$$

$$a_4 = \frac{\delta}{\alpha} - 1\,, \quad a_5 = \frac{\Delta t}{2}\left(\frac{\delta}{\alpha} - 2\right), \quad a_6 = \Delta t\,(1-\delta)\,, \quad a_7 = \delta\,\Delta t \tag{13}$$

and the effective stiffness matrix (coefficient matrix)

$$\hat{\mathbf{K}} = \mathbf{K} + a_0\,\mathbf{M} + a_1\,\mathbf{D} \tag{14}$$

as well as the effective load vector

$$\hat{\mathbf{R}}_{t+\Delta t} = \mathbf{R}_{t+\Delta t} + \mathbf{M}\,(a_0\,\mathbf{u}_t + a_2\,\dot{\mathbf{u}}_t + a_3\,\ddot{\mathbf{u}}_t) + \mathbf{D}\,(a_1\,\mathbf{u}_t + a_4\,\dot{\mathbf{u}}_t + a_5\,\ddot{\mathbf{u}}_t)\,, \tag{15}$$

Algorithm 1 Computation sequence

for train i of train set **do**
  for LC j of LC set **do**
    for range of $60\,\mathrm{km/h} \leq v \leq 1.2\,v_{\mathrm{train,design}}$ **do**
      for range of $1\,\mathrm{m} \leq L \leq 120\,\mathrm{m}$ **do**
        ▶ transient time-step integration (static/dynamic)
        ▶ compute S_{stat} at mid-span
        ▶ compute S_{dyn} at mid-span
        ▶ compute part of track irregularities $0.5\,\varphi''\,S_{\mathrm{stat}}$ at mid-span
        ▶ compute objective quantities $\lambda_{\mathrm{ULS,dyn}}$, a_z, $u_{z,\mathrm{dyn}}$, $a_{z,\mathrm{eff}}$, $\lambda_{\mathrm{fat,dyn}}$, $1+\varphi'_{\mathrm{dyn}}$
      end for
    end for
    ▶ post-processing: output permissible max v_{perm} train i for LC j
  end for
end for

the equation of motion is solved in an iterative manner,

$$\hat{\mathbf{K}}\,\mathbf{u}_{t+\Delta t} = \hat{\mathbf{R}}_{t+\Delta t}\,, \tag{16}$$

by iteratively updating the acceleration

$$\ddot{\mathbf{u}}_{t+\Delta t} = a_0\,(\mathbf{u}_{t+\Delta t} - \mathbf{u}_t) - a_2\,\dot{\mathbf{u}}_t - a_3\,\ddot{\mathbf{u}}_t \tag{17}$$

and velocity

$$\dot{\mathbf{u}}_{t+\Delta t} = \dot{\mathbf{u}}_t + a_6\,\ddot{\mathbf{u}}_t + a_7\,\ddot{\mathbf{u}}_{t+\Delta t} \tag{18}$$

at time $t+\Delta t$. In the case of the non-linear calculation (NL), Eq. (16) is iteratively solved after linearization of the modal DOF-dependent damping matrix in each time step using the Newton-Raphson method. The calculation algorithm with the individual solution steps is shown in algorithmic form in Alg. 1. The implementation was verified by comparison with a reference software for the case of the L-calculation.

In Alg. 1, it can be seen that a speed range for the train passage is evaluated in each case up to the train design velocity, extended by the safety factors 1.2 (ULS) and 1.1 (SLS, FAT) in order to take account of slightly shifted natural frequencies of the bridge structures in reality as well as deviations in normal operation (local train speed).

The following objective quantities are computed from the dynamically determined internal forces/moments S evaluated at mid-span (simplification). As part of the ULS assessment, the dynamic action is normalized to the internal static moments/forces caused by the LM71 load model with

$$\lambda_{\mathrm{ULS,dyn}} = \frac{S_{\mathrm{dyn}} + 0.5\,\varphi''\,S_{\mathrm{stat}}}{\Phi_2\,S_{\mathrm{stat,LM71}}} \tag{19}$$

taking into account carefully maintained tracks ($a_0 = 0.5$, Φ_2). For the assessment of the SLS, the value

$$a_z = \max(\mathrm{abs}(\ddot{u}(t))) \tag{20}$$

is used. Furthermore, a so-called "effective" acceleration is proposed and also computed by weighting the acceleration value via the max. amplitude of the displacement of the vibration

and a static reference value $L/200$ (must be discussed further),

$$a_{z,\mathrm{eff}} = a_z \, \frac{u_{\mathrm{dyn}}}{L/200} \, . \tag{21}$$

For the evaluation of the dynamic fatigue effect of the train on the bridge, a dynamic quantity $\lambda_{\mathrm{fat,dyn}}$ corresponding to DIN EN 1993-2:2010 is calculated by evaluating the stress amplitudes in relation to LM71 with an equivalent number of cycles (25 million tons per year, 100 years of service life)

$$\lambda_{\mathrm{fat,dyn}} = \frac{\Delta\sigma_{\mathrm{E,2,dyn}}}{\Phi_2 \, \Delta\sigma_{\mathrm{LM71}}} \, . \tag{22}$$

Here, the equivalent dynamic stress range $\Delta\sigma_{\mathrm{E,2,dyn}}$ for 2 million load cycles is determined by taking into account the evaluation of the Wöhler line of the respective design for dynamic internal forces/moments with added part of track irregularities. As alternative criterion for the fatigue effect, the measure

$$1 + \varphi'_{\mathrm{dyn}} = \frac{S_{\mathrm{dyn}}}{S_{\mathrm{stat}}} \tag{23}$$

according to DB-Ril 804.3301 is computed as well. The evaluation of the objective values is also summarized in Alg. 1.

Regarding the infrastructure capacity, the limit values for the ULS are

$$\lambda_{\mathrm{LC}}(v_{\mathrm{infra}}, L) = \frac{S_{\mathrm{quasi\text{-}static,LC}}}{\Phi_2 \, S_{\mathrm{stat,LM71}}} = \frac{(1 + \varphi' + 0.5\,\varphi'') \, S_{\mathrm{stat,LC}}}{\Phi_2 \, S_{\mathrm{stat,LM71}}} = \frac{(1 + \varphi' + 0.5\,\varphi'')}{\Phi_2} \, \lambda_{\mathrm{stat,LC}} \tag{24}$$

with the local speed of the infrastructure and the static value of the line category $\lambda_{\mathrm{stat,LC}}$ of the respective LC (evaluation of reference trains according to DIN EN 15528:2022 or national extensions of LC, e.g. D4DB for German railway network). Then, $\lambda_{\mathrm{ULS,dyn}}$ of the train in the speed range of $60\,\mathrm{km/h} \leq v \leq 1.2\,v_{\mathrm{train,design}}$ is evaluated and compared step by step. In the SLS, compliance with the limit value of $3.5\,\mathrm{m/s^2}$ is checked for $L > 7\,\mathrm{m}$. In the fatigue limit (FAT), the limit criterion $\lambda_{\mathrm{fat,dyn}} \leq 1.4$ is evaluated for the calculated values of the action of the train for all spans as well as the additional criterion $1 + \varphi'_{\mathrm{dyn}} \leq 1.5$ (DB-Ril 804.3301).

By gradually increasing the train velocity v as part of the parameter study over the range L and v (see Alg. 1), the permissible speeds according to the respective limit states (taking into account the respective partial safety factor for the speed) can be identified by the first exceedance. The permissible speeds are determined in the following section for selected, exemplary representatives of two train types.

5 RESULTS AND DISCUSSION: PARAMETER STUDIES

The above-described procedure for verifying the dynamic bridge compatibility of new vehicles/trains on the railway network (Germany) was applied to two representative trains (long-distance Train A (locomotive + 8 coaches, $v_{\mathrm{train,design}} = 200\,\mathrm{km/h}$, train LC: D2) and regional Train B (multiple-unit train of 3 units, $v_{\mathrm{train,design}} = 160\,\mathrm{km/h}$, train LC: D2) with their train-specific maximum design velocities (operational speed). First, the objective values from the parameter study were determined using the calculation modes L and NL, see Fig. 7.

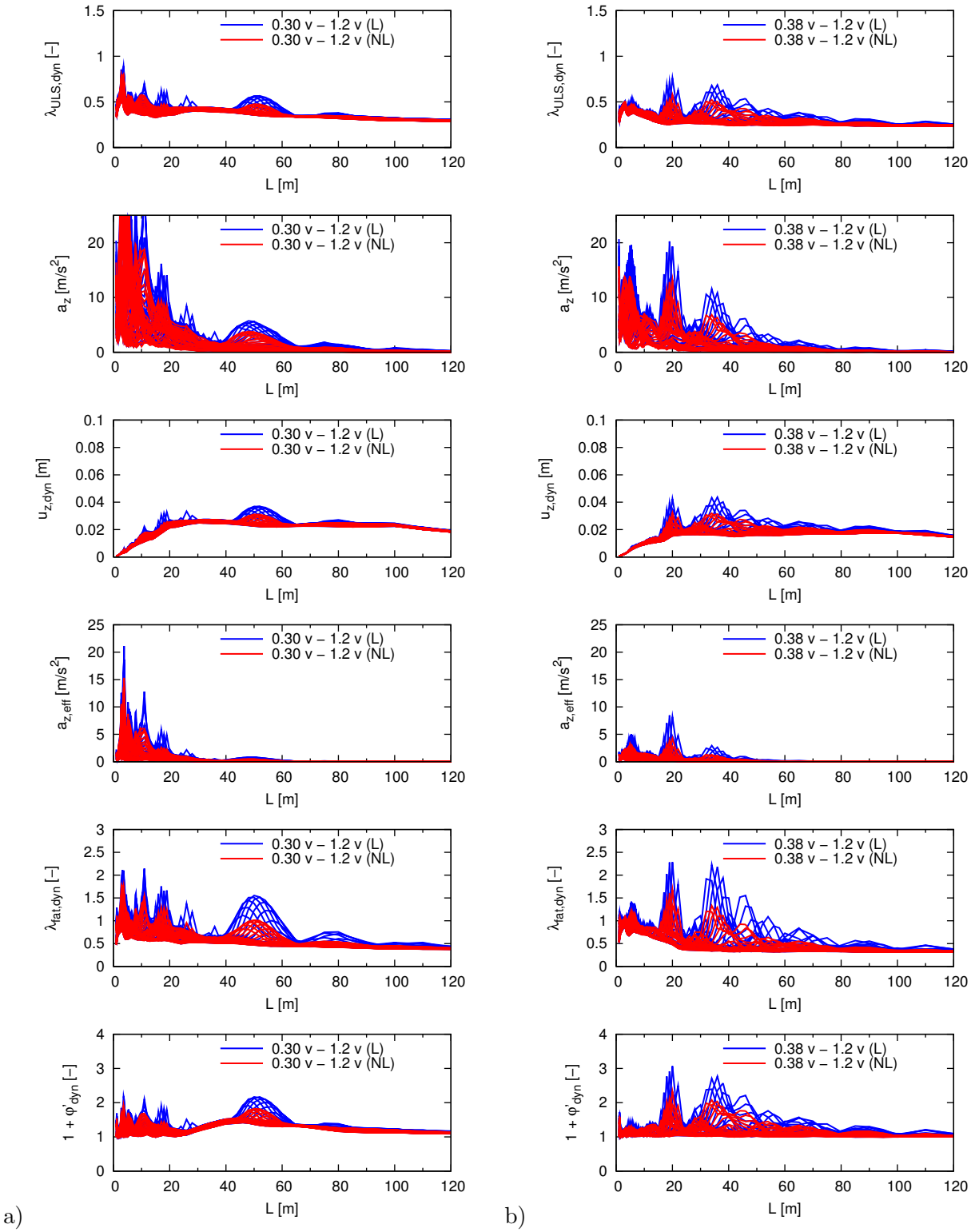

Figure 7: Parameter study results ($\Delta v = 5\,\mathrm{km/h}$) – objective quantities: a) Train A, b) Train B

Table 1: Results: base speed for linear and non-linear analysis Level 2 for selected Trains A and B

Train A		**L**			**NL**		
$\mathbf{LC}_{\text{infrastructure}}$		**D2**	**D4**	**D4DB**	**D2**	**D4**	**D4DB**
$v_{\text{B}}(\lambda_{\text{ULS}})$	[km/h]	54.2	54.2	195.8	195.8	195.8	200.0
$v_{\text{B}}(a_z)$	[km/h]	59.1	59.1	59.1	72.7	72.7	72.7
$v_{\text{B}}(a_{z,\text{eff}})$	[km/h]	118.2	118.2	118.2	200.0	200.0	200.0
$v_{\text{B}}(\lambda_{\text{fat}})$	[km/h]	118.2	118.2	118.2	200.0	200.0	200.0
$v_{\text{B}}(1+\varphi'_{\text{dyn}})$	[km/h]	118.2	118.2	118.2	181.8	181.8	181.8

Train B		**L**			**NL**		
$\mathbf{LC}_{\text{infrastructure}}$		**D2**	**D4**	**D4DB**	**D2**	**D4**	**D4DB**
$v_{\text{B}}(\lambda_{\text{ULS}})$	[km/h]	116.7	160.0	160.0	160.0	160.0	160.0
$v_{\text{B}}(a_z)$	[km/h]	63.6	63.6	63.6	77.3	77.3	77.3
$v_{\text{B}}(a_{z,\text{eff}})$	[km/h]	118.1	118.1	118.1	127.3	127.3	127.3
$v_{\text{B}}(\lambda_{\text{fat}})$	[km/h]	118.2	118.2	118.2	127.3	127.3	127.3
$v_{\text{B}}(1+\varphi'_{\text{dyn}})$	[km/h]	81.8	81.8	81.8	100.0	100.0	100.0

Subsequently, the max. base speeds v_{B} for different LC, i.e. different infrastructure capacities, were determined in a post-processing calculation. Due to the dependence on the load capacity $\lambda_{\text{stat,LC}}$, this is only relevant for the ULS. The other base speeds obtained for the SLS and FAT cases are independent of the underlying LC of the infrastructure in the procedure shown here.

From the comparison of the determined velocities, see Tab. 1, it can be concluded that potential reserves exist when applying the NL-calculation and that these lead to higher permissible base velocities per LC. This applies to ULS, SLS and FAT, as the dynamic peak amplitudes in the resonance case are reduced for all cases and are significantly lower than those of the L-calculation (compare the results of the parameter study shown in Fig. 7). The results shown here still need to be experimentally validated and transferred to a standardized approach. This is currently the subject of an EU-wide research project that aims to identify reserves within the acceleration limits and damping values.

6 HOMOGENIZATION ON THE EUROPEAN SCALE

The InBridge4EU project is currently working with partner institutions across Europe to develop new recommendations for the European standards for train-bridge interaction. The procedure shown here can be used to determine revised, adapted limit speeds in analogy to DIN EN 15528:2022, Table C.1. For this purpose, A) the underlying model assumptions of non-linearity must first be validated experimentally, B) the limits of the acceleration must be checked experimentally, C) the underlying database must be expanded at European level (bridge stock and national particularities) and D) the calculation procedure in Alg. 1 must be used for identified representative train families (as a function of dynamic train categories or vehicle LC and vehicle type) to derive stochastic limit speeds per train from the results for each representative train family.

7 CONCLUSIONS

In this contribution, an evaluation method for new vehicles was presented that allows the infrastructure-dependent base speed for network-wide access to be determined in the context of dynamic vehicle-bridge compatibility (Level 2). It could be shown that the non-linear modeling of damping values based on the findings available from measurement series on a large number of measured existing bridges can open up reserves or clarify the gap between previously calculated low base speeds (L) and higher speeds observed for existing (former) vehicles, which are generally not linked to any damage reports during regular bridge inspections. The presented evaluation method might be extended to other underlying static systems (continuous beam, sophisticated spatial models), which can be studied by the general FE method.

ACKNOWLEDGEMENT

Parts of the research reported herein have been carried out within the EU research project InBridge4EU. The funding received from the Europe's Rail Joint Undertaking under Horizon Europe research and innovation program under grant agreement No. 101121765 (HORIZON-ER-JU-2022-ExplR-02) is gratefully acknowledged.

REFERENCES

[1] Bathe, K.-J. 1996. "Finite Element Procedures." Prentice-Hall, Englewood Cliffs, 1996.

[2] Behnke, R., G. Grunert, X. Liu 2023. "Bewertung der fahrzeugspezifischen Ermüdungseinwirkung auf Bestandsbrücken bei Zugüberfahrt." 18. D-A-CH-Tagung, Erdbebeningenieurwesen und Baudynamik: 329–336, Kiel, Germany.

[3] Grunert, G. 2022. "Data and Evaluation Model for the Description of the Static–dynamic Interface Between Trains and Railway Bridges." Eng. Struct. 262: 114335. https://doi.org/10.1016/j.engstruct.2022.114335

[4] Kang, C., S. Schneider, M. Wenner, S. Marx 2018. "Development of Design and Construction of High-speed Railway Bridges in Germany." Eng. Struct. 163: 184–196. https://doi.org/10.1016/j.engstruct.2018.02.059

[5] Montenegro, P. A., H. Carvalho, D. Ribeiro, R. Calçada, M. Tokunaga, M. Tanabe, W. M. Zhai 2021. "Assessment of Train Running Safety on Bridges: A Literature Review." Eng. Struct. 241: 112425. https://doi.org/10.1016/j.engstruct.2021.112425

[6] Szafrański, M. 2021. "A Dynamic Vehicle-Bridge Model Based on the Modal Identification Results of an Existing EN57 Train and Bridge Spans with Non-ballasted Tracks." Mech. Syst. Signal Process. 146: 107039. https://doi.org/10.1016/j.ymssp.2020.107039

[7] Tahiri, M., A. Khamlichi, M. Bezzazi 2022. "Nonlinear Analysis of the Ballast Influence on the Train-Bridge Resonance of a Simply Supported Railway Bridge." Structures 35: 303–313. https://doi.org/10.1016/j.istruc.2021.11.020

[8] Yang, Y. B., J. D. Yau 2017. "Resonance of High-speed Trains Moving Over a Series of Simple or Continuous Beams with Non-ballasted Tracks." Eng. Struct. 143: 295–305. https://doi.org/10.1016/j.engstruct.2017.04.022